Error rate analysis of MDPSK/CPSK with diversity reception under very slow Rayleigh fading and cochannel interference

doi: 10.1109/25.293643

Error Rate Analysis of MDPSK/CPSK with Diversity Reception Under Very Slow Rayleigh Fading and Cochannel Interference

Fumiyuki Adachi, *Senior Member, IEEE,* and Mamoru Sawahashi, *Member, IEEE*

Abstract—**The distribution of the phase noise due to additive white Gaussian noise (AWGN) and cochannel interference (CCI) is analyzed for differential phase detection (DPD) and coherent phase detection (CPD) in a very slow nonfrequency selective Rayleigh fading environment. The effects of modulation timing offset between the desired signal and the CCI and of the overall channel filter response are considered. Simple closed-form expressions are derived for ideal selection diversity reception. The derived phase noise distributions are used for evaluating the bit error rate (BER) performance of 2-16DPSK/CPSK assuming square-root raised cosine Nyquist transmit/receive filters. It is found that the BER performance of CPSK is less sensitive to CCI modulation timing offset than DPSK, and that increasing the filter rolloff factor can improve the BER performance due to CCI. Finally, the accuracy of the BER approximation that uses the symbol error rate is discussed.**

I. Introduction

LINEAR multilevel DPSK/CPSK modulation is attracting more and more attention in the field of mobile radio because it requires a much narrower bandwidth than does constant envelope digital FM. The decision on which symbol was transmitted can be performed based on the phase change of the received signal over one symbol period for DPSK and the phase difference between the received signal and regenerated noise-free reference signal for CPSK. The error rates of MDPSK/CPSK in an additive white Gaussian noise (AWGN) channel, therefore, can be evaluated using the phase noise distribution derived by Pawula *et al.* [1], [2] (note that for 4-level modulation, a simple binary decision on the in-phase and quadrature phase outputs of the quadrature differential/coherent detector can be employed). In mobile radio, AWGN is not the only cause of errors. The fading-induced random phase noise (or often referred to as random FM noise) and multipath channel delay spread also cause errors. These two determine the range of available transmission bit rates in fading environments; errors are caused predominantly by the former for low bit rate transmissions and by the latter for high bit rate transmissions. For cellular systems, the same radio frequencies are reused at spatially separated cells in order to efficiently utilize the limited radio spectrum resources, thereby producing cochannel interference (CCI). The CCI performance determines the reuse distance of the same radio frequency and thus affects spectrum efficiency [4]–[6]. Hence the most important subject is CCI performance. Since both the desired signal and CCI are subjected to fading, the error rates due to CCI are significantly increased compared with the non fading case. Diversity reception can be used to combat the fading effect [3].

Miyagaki *et al.* [7] derived the probability density function (pdf) of the differential phase noise of a Rayleigh faded signal corrupted by AWGN and investigated the average symbol error rates of MDPSK. Pauw and Schilling [8] applied Pawula *et al.*'s approach [1] to derive the phase noise distributions due to AWGN under very slow nonfrequency selective Rayleigh fading and evaluated the error rates of both MDPSK and MCPSK. However, no previous analysis [7], [8] has considered CCI and diversity reception. Recently, Adachi and Sawahashi [9] extended Pauw and Schilling's analysis [8] to include selection diversity reception. Proakis [10] described adaptive diversity reception which is a type of maximal-ratio combining. However, none of the previous papers [7]–[10] took into account CCI (note that for the 4DPSK case several papers can be found [11]–[13]).

In this paper, we investigate MDPSK/CPSK error rate performance with selection diversity reception in the presence of Rayleigh fading and CCI. We consider the modulation timing offset between the desired signal and CCI, as well as the transmission channel filter response. Among several diversity combining schemes, selection combining, which chooses the branch having the largest instantaneous received signal power, is the simplest and is considered to be the most practical. Our analysis neglects the effects of fading-induced random phase noise and delay spread, i.e., very slow nonfrequency selective fading is assumed. The paper is organized as follows. Section II describes the transmission system model. The closed-form expressions for the phase noise distribution are derived for differential phase detection (DPD) and coherent phase detection (CPD) in Sections III and IV, respectively. In Section V, the distributions for the special cases of AWGN-limited channel, CCI-limited channel, and unmodulated CCI are discussed. The derived phase noise distributions are used to calculate the bit error rates (BER's) of 2-16DPSK/CPSK assuming square-root raised cosine Nyquist transmit/receive filters. The impact of the CCI modulation timing offset and

Manuscript received June 23, 1992; revised October 5, 1992 and August 2, 1993.

The authors are with R&D Department, NTT Mobile Communications Network, Inc., Kanagawa-Ken, 238 Japan.

IEEE Log Number 9213787.

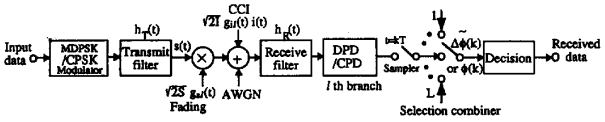

Fig. 1. Transmission model.

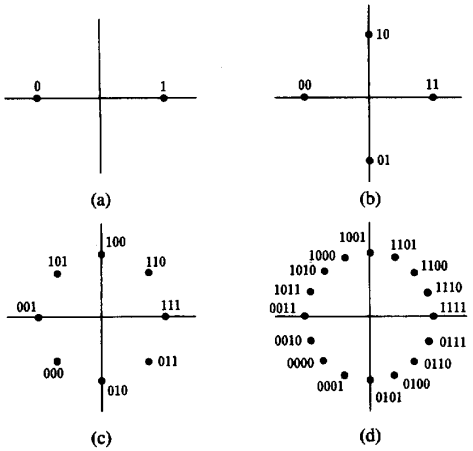

Fig. 2. Signal Constellations. (a) 2 PSK. (b) 4 PSK. (c) 8 PSK. (d) 16 PSK.

the filter rolloff factor on the BER performance are discussed in Section VI. Also discussed is the accuracy of the BER approximation.

II. Transmission System Model

Fig. 1 shows the transmission model. Signal constellations with Gray encoding are shown in Fig. 2 (the constellations for MDPSK are shown in the differential phase plane). The kth symbol ($\log_2 M$-bit) to be transmitted is mapped to the phase $\phi_s(k)$ of the carrier for MCPSK and to the differential phase $\Delta\phi_s(k) = \phi_s(k) - \phi_s(k-1)$ for MDPSK, where $\Delta\phi_s(k)$ takes on one of the M values from the set $\{2m\pi/M; m = -M/2, \pm(M/2-1), \cdots, \pm 1, 0\}$ as does $\phi_s(k)$. The filtered transmitted signal is represented as

$$s(t) = \sum_{k=-\infty}^{\infty} \exp[j\,\phi_s(k)] h_T(t - kT) \qquad (1)$$

where $h_T(t)$ is the baseband equivalent transmit filter impulse response with $1/T \int_{-\infty}^{\infty} |h_T(t)|^2 dt = 1$ and T is the symbol duration.

The received desired signal is corrupted by AWGN and CCI. We assume that both the desired signal and the CCI are MDPSK (or MCPSK) modulated by different symbol sequences with different modulation timing. Since the CCI is from a spatially separated cell, its multipath channel is different from that of the desired channel, and thus we can assume mutually independent Rayleigh fading for the desired signal and the CCI. Ideal L-branch selection diversity reception is considered. The baseband equivalent complex envelope $r(t)$ for any of the L branches can be written (the branch number $l(=1,2,\cdots,L)$ is omitted for simplicity) as

$$r(t) = \sqrt{2S}\, g_s(t) s(t) + \sqrt{2I}\, g_i(t) i(t) + \text{AWGN} \qquad (2)$$

where $i(t)$ is the CCI signal representation and can be expressed similarly to (1) as

$$i(t) = \sum_{k=-\infty}^{\infty} \exp[j\,\phi_i(k)] h_T(t + \Delta T - kT) \qquad (3)$$

where ΔT is the modulation timing offset ($-T/2 \leqq \Delta T < T/2$). Terms $g_s(t)$ and $g_i(t)$ are mutually independent zero-mean complex Gaussian processes with unity variance ($<|g_s(t)|^2> = <|g_i(t)|^2> = 1$). S and I are the average powers of the desired signal and the CCI, respectively. The power spectra of $g_s(t)$ and $g_i(t)$ are confined within $\pm f_D$ Hz, where f_D is the maximum Doppler frequency given by mobile station travelling speed/carrier wavelength.

The received signal $r(t)$ is bandlimited by the receive filter. We assume very slow fading such that the fading complex envelope remains almost constant over several symbol periods. This holds only if the maximum Doppler frequency $f_D T$, normalized by the symbol rate, is very small. This assumption is valid in most practical situations. For example, assuming a 1-GHz carrier frequency and 100-km/h traveling speed, f_D is 92.6 Hz. If the symbol rate $1/T$ is larger than 10 k symbol/s, then $f_D T < 0.01$. It was shown [12] that at this value of $f_D T$, the irreducible BER of 4DPSK due to random phase noise can be reduced to nearly 10^{-6} by simple two-branch diversity reception. For such very slow fading, therefore, we can neglect the time dependence of $g_s(t)$ and $g_i(t)$ during a time interval over several symbol periods, and the receive filter output can be expressed as

$$\tilde{r}(t) = \sqrt{2S}\, g_s d_s(t) + \sqrt{2I}\, g_i d_i(t) + n(t) \qquad (4)$$

where $d_s(t)$ and $d_i(t)$ are the receive filter responses to $s(t)$ and $i(t)$, respectively, and $n(t)$ is the bandpass-filtered AWGN component with power $1/2<|n(t)|^2> = N$. The overall (transmit and receive) filter response is $h(t) = h_T(t) * h_R(t)$, where $h_R(t)$ is the baseband equivalent impulse response of the receive filter and $*$ is the convolution operation. We assume here a square root Nyquist filter (i.e., $h_T(t) = T h_R(t)$) at the transmitter and receiver so that $h(kT) = 0$ if $k \neq 0$ and $h(0) = 1$. Furthermore, we assume that the sampling timing is ideally locked to the desired signal timing (this assumption is valid for large signal-to-AWGN plus CCI power ratio (SNIR)). The receive filter output at $t = kT$ is, therefore,

$$\begin{aligned}\tilde{r}(k) &= \sqrt{2S}\, g_s \exp j\,\phi_s(k) + \sqrt{2I}\, g_i d_i(k) + n(k) \\ &= R(k) \exp j\,[\phi_s(k) + \theta(k) + \mu] \end{aligned} \qquad (5)$$

where $R(k), \theta(k)$, and $\mu\,(= \arg g_s)$ are the envelope, phase noise due to AWGN plus CCI, and fading-induced random

phase, respectively, and

$$d_i(k) = \sum_{m=-\infty}^{\infty} \exp[j\,\phi_i(k+m)]h(\Delta T - mT). \quad (6)$$

DPD and CPD are assumed for detection of MDPSK and MCPSK signals, respectively. The reference signal for CPD is assumed to ideally track the fading-induced random phase variations of the desired signal and, therefore, its complex envelope is given by g_s. The detector outputs can be represented as

$$\Delta\tilde{\phi}(k) = \arg[\tilde{r}(k)\tilde{r}^*(k-1)] = \Delta\phi_s(k) + \Delta\theta(k) \quad \text{for DPD}$$
$$\tilde{\phi}(k) = \arg[\tilde{r}(k)g_s^*] = \phi_s(k) + \theta(k) \quad \text{for CPD} \quad (7)$$

where $\Delta\theta(k)(=\theta(k) - \theta(k-1))$ and $\theta(k)$ are the phase noises for DPD and CPD, respectively. They are distributed over $[-\pi, \pi)$ due to AWGN plus CCI. Decision error is caused when $|\Delta\theta(k)| > \pi/M$ for DPD and $|\theta(k)| > \pi/M$ for CPD. The error rates can, therefore, be evaluated using the distributions of $\Delta\theta(k)$ and $\theta(k)$ (hereafter, we simply refer to these as $\Delta\theta$ and θ).

So far, we have described the single branch case. For L-branch selection diversity, branch selection is assumed to be done after phase detection so that the phase discontinuity which may cause decision errors can be avoided. The detector output of the branch having the largest instantaneous desired signal power $S|g_s|^2$ is chosen.

III. DPD Phase Noise Distribution

A. Statistical Properties of Detector Input

For the given $d_i(k)$ (or equivalently for the given sequence of $\boldsymbol{\phi}_i = (\cdots\phi_i(k-2), \phi_i(k-1), \phi_i(k), \phi_i(k+1), \phi_i(k+2)\cdots)$ and the modulation timing offset ΔT, the Rayleigh faded CCI is a zero-mean complex Gaussian variable; therefore, AWGN plus faded CCI can be treated as an additive complex Gaussian noise. This implies that the phase noise distribution can be derived based on Pawula *et al.*'s approach described in [1]. First we derive the conditional phase noise distribution when the desired signal complex envelope = g_s (or the instantaneous power = $S|g_s|^2$), and then we perform averaging over the statistics of $S|g_s|^2$. For derivation of the conditional phase noise distribution, we need the conditional signal-to-AWGN plus CCI power ratio (SNIR) $\rho(k)$ and noise correlation $r + j\lambda$ between $\tilde{r}(k)$ and $\tilde{r}(k-1)$. The SNIR is defined as the ratio of the desired signal instantaneous power to the ensemble average of AWGN plus CCI power for the given $\boldsymbol{\phi}_i$ and ΔT. The ensemble average of AWGN plus CCI power is given by $P = 1/2<|\sqrt{2I}g_i d_i(k) + n(k)|^2> = I \times |d_i(k)|^2 + N$ and

$$\rho(k) = \frac{S|g_s|^2}{I|d_i(k)|^2 + N} = \alpha^2(k)\gamma \quad (8)$$

where $\gamma = (S/N)|g_s|^2$ is the instantaneous desired signal-to-AWGN power ratio (SNR) and

$$\alpha^2(k) = \frac{\Lambda}{\Gamma|d_i(k)|^2 + \Lambda} \quad (9)$$

with $\Gamma(=S/N)$ and $\Lambda(=S/I)$ being the average SNR and average desired signal-to-CCI power ratio (SIR), respectively. Since we are assuming a square root Nyquist receive filter, the filtered AWGN samples are statistically independent, and $r + j\lambda$ is given by (10).

B. Conditional Phase Noise Distribution

In general, $\rho(k) \neq \rho(k-1)$ and $r + j\lambda \neq 0$. We apply Pawula *et al.*'s case 3—unequal signal condition, correlated noises [1] to our case. The phase noise $\Delta\theta$ is defined over the range of $[-\pi, \pi)$. When $r + j\lambda \neq 0$, the phase noise distribution is affected not only by $\boldsymbol{\phi}_i$ and ΔT but also by the desired signal modulation $\Delta\phi_s$. The conditional distribution of $\Delta\theta$ with $\gamma, \Delta\phi_s, \boldsymbol{\phi}_i$ and ΔT being given can be expressed as

$$p(\psi|\gamma, \Delta\phi_s, \boldsymbol{\phi}_i, \Delta T) = \Pr[-\pi \le \Delta\theta \le \psi|\gamma] = F(\psi|\gamma, \Delta\phi_s, \boldsymbol{\phi}_i, \Delta T) - F(-\pi|\gamma, \Delta\phi_s, \boldsymbol{\phi}_i, \Delta T) + U(\psi) \quad (11)$$

$$r + j\lambda = \frac{\frac{1}{2}\langle(\sqrt{2I}g_i d_i(k) + n(k))(\sqrt{2I}g_i d_i(k-1) + n(k-1))^*\rangle}{\sqrt{I|d_i(k)|^2 + N}\sqrt{I|d_i(k-1)|^2 + N}} = \alpha(k)\,\alpha(k-1)\frac{\Gamma\, d_i(k)d_i^*(k-1)}{\Lambda} \quad (10)$$

$$F(\psi|\gamma, \Delta\phi_s, \boldsymbol{\phi}_i, \Delta T) = \int_{-(\pi/2)}^{(\pi/2)} dt \frac{e^{-E}}{4\pi} \cdot \left[\frac{-W\sin\psi}{U - V\sin t - W\cos\psi\cos t} + \frac{r\sin(\psi + \Delta\phi_s) - \lambda\cos(\psi + \Delta\phi_s)}{1 - \{r\cos(\psi + \Delta\phi_s) + \lambda\sin(\psi + \Delta\phi_s\}\cos t}\right] \quad (12a)$$

$$E = \frac{U - V\sin t - W\cos\psi\cos t}{1 - \{r\cos(\psi + \Delta\phi_s) + \lambda\sin(\psi + \Delta\phi_s)\}\cos t} \quad (12b)$$

where $U(\psi) = 0$ if $\psi \leq 0$ and 1 otherwise, and $F(\psi|\gamma, \Delta\phi_s, \boldsymbol{\phi}_i, \Delta T)$ is given by (12). U, V, W, and $r + j\lambda$ are the same notations as used in [1, eq. (12)]; however, in our case, the SNR ρ used in U, V, and W of [1] is replaced with the conditional SNIR and ψ with $\psi + \Delta\phi_s$ to make ψ-range form $-\pi$ to π. U, V, and W are then

$$U = \frac{1}{2}[\rho(k) + \rho(k-1)] = \gamma \frac{\alpha^2(k) + \alpha^2(k-1)}{2} \quad (13a)$$

$$V = \frac{1}{2}[\rho(k) - \rho(k-1)] = \gamma \frac{\alpha^2(k) - \alpha^2(k-1)}{2} \quad (13b)$$

$$W = \sqrt{\rho(k)\,\rho(k-1)} = \gamma\,\alpha(k)\,\alpha(k-1). \quad (13c)$$

Letting $U = \gamma u$, $V = \gamma v$, and $W = \gamma w$, $F(\psi|\gamma, \Delta\phi_s, \boldsymbol{\phi}_i, \Delta T)$ can be rewritten as (14).

C. Phase Noise Distribution

From (11), the phase noise distribution under Rayleigh fading can be expressed as

$$P(\psi|\Delta\phi_s, \boldsymbol{\phi}_i, \Delta T) = \overline{F}(\psi|\Delta\phi_s, \boldsymbol{\phi}_i, \Delta T) - \overline{F}(-\pi|\Delta\phi_s, \boldsymbol{\phi}_i, \Delta T) + U(\psi) \quad (15)$$

where

$$\overline{F}(\psi|\Delta\phi_s, \boldsymbol{\phi}_i, \Delta T) = \int_0^\infty F(\psi|\gamma, \Delta\phi_s, \boldsymbol{\phi}_i, \Delta T) p(\gamma)\, d\gamma \quad (16)$$

is the average of $F(\psi|\gamma, \Delta\phi_s, \boldsymbol{\phi}_i, \Delta T)$ using the pdf of γ with selection diversity reception which is given by [3]

$$p(\gamma) = \frac{L}{\Gamma} \exp\left(-\frac{\gamma}{\Gamma}\right)\left[1 - \exp\left(-\frac{\gamma}{\Gamma}\right)\right]^{L-1} = \frac{L}{\Gamma} \sum_{l=0}^{L-1} \binom{L-1}{l} (-1)^l \exp\left[-\frac{\gamma}{\Gamma}(1+l)\right]. \quad (17)$$

From (18), $\overline{F}(\psi|\Delta\phi_s, \boldsymbol{\phi}_i, \Delta T)$ becomes (19). Using (A1) and $u^2 - v^2 = w^2$ (see (13)), the first integral in (19) becomes

$$I_1 = -\frac{\operatorname{sgn}\psi}{\pi} \tan^{-1} \sqrt{\frac{1 + \cos\psi}{1 - \cos\psi}} = \frac{-\operatorname{sgn}\psi}{2}\left(1 - \frac{|\psi|}{\pi}\right). \quad (20)$$

For the second integral, we use again (A1) with (21) to obtain

$$I_2 = \frac{-1}{\pi} \frac{\operatorname{Im}(\eta_l \exp -j\psi)}{\sqrt{1 - \operatorname{Re}^2(\eta_l \exp -j\psi)}} \cdot \tan^{-1} \sqrt{\frac{1 + \operatorname{Re}(\eta_l \exp -j\psi)}{1 - \operatorname{Re}(\eta_l \exp -j\psi)}} \quad (22)$$

$$F(\psi|\gamma, \Delta\phi_s, \boldsymbol{\phi}_i, \Delta T) = \frac{1}{4\pi} \int_{-(\pi/2)}^{(\pi/2)} dt \exp \cdot \left[-\gamma \frac{u - \nu \sin t - w \cos\psi \cos t}{1 - \{r\cos(\psi + \Delta\phi_s) + \lambda \sin(\psi + \Delta\phi_s)\}\cos t}\right] \times \left[\frac{-w \sin\psi}{u - \nu \sin t - w\cos\psi \cos t} + \frac{r\sin(\psi + \Delta\phi_s) - \lambda\cos(\psi + \Delta\phi_s)}{1 - \{r\cos(\psi + \Delta\phi_s) + \lambda \sin(\psi + \Delta\phi_s)\}\cos t}\right] \quad (14)$$

$$\frac{1}{\Gamma}\int_0^\infty \exp\left[-\frac{\gamma}{\Gamma}(1+l) - \gamma \frac{u - \nu\sin t - w\cos\psi\cos t}{1 - \{r\cos(\psi + \Delta\phi_s) + \lambda\sin(\psi + \Delta\phi_s)\}\cos t}\right] dt = \frac{1 - \{r\cos(\psi + \Delta\phi_s) + \lambda\sin(\psi + \Delta\phi_s)\}\cos t}{(1+l)[1 - \{r\cos(\psi + \Delta\phi_s) + \lambda\sin(\psi + \Delta\phi_s)\}\cos t] + \Gamma(u - \nu\sin t - w\cos\psi\cos t)} \quad (18)$$

$$\overline{F}(\psi|\Delta\phi_s, \boldsymbol{\phi}_i, \Delta T) = L \sum_{l=0}^{L-1} \binom{L-1}{l} \frac{(-1)^l}{1+l} \cdot \int_{-(\pi/2)}^{+(\pi/2)} \frac{1}{4\pi} dt \left[\frac{-w\sin\psi}{u - \nu\sin t - w\cos\psi\cos t} + \frac{w\sin\psi + \frac{1+l}{\Gamma}\{r\sin(\psi + \Delta\phi_s) - \lambda\cos(\psi + \Delta\phi_s)\}}{u + \frac{1+l}{\Gamma} - \nu\sin t - \left[w\cos\psi + \frac{1+l}{\Gamma}\{r\cos(\psi + \Delta\phi_s) + \lambda\sin(\psi + \Delta\phi_s)\}\right]\cos t}\right] \quad (19)$$

where

$$\eta_l = \frac{w + \frac{1+l}{\Gamma}(r + j\lambda)\exp -j\Delta\phi_s}{\sqrt{w^2 + 2u\frac{1+l}{\Gamma} + \left(\frac{1+l}{\Gamma}\right)^2}} = \frac{\alpha(k)\alpha(k-1) + \frac{1+l}{\Lambda}(r + j\lambda)\exp -j\Delta\phi_s}{\sqrt{\alpha^2(k) + \frac{1+l}{\Gamma}}\sqrt{\alpha^2(k-1) + \frac{1+l}{\Gamma}}}. \quad (23)$$

Equation (23) was obtained from $u = (\alpha^2(k) + \alpha^2(k-1))/2$ and $w = \alpha(k)\alpha(k-1)$ (see (13)). Substituting (20) and (22) into (19) and using

$$\sum_{l=0}^{n} \frac{(-1)^l}{1+l}\binom{n}{l} = \frac{1}{n+1} \quad (24)$$

we have (25). Finally, substituting (25) into (15), we obtain (26). An alternative expression can be found from (A2) as found in (27). $\alpha(k)$ and $r + j\lambda$ are defined in (9) and (10), respectively. η_l can be rewritten

$$\eta_l = \frac{1 + \frac{1+l}{\Lambda}d_i(k)d_i^*(k-1)\exp -j\Delta\phi_s}{\sqrt{1+(1+l)\left[\frac{1}{\Gamma} + \frac{|d_i(k)|^2}{\Lambda}\right]}\sqrt{1+(1+l)\left[\frac{1}{\Gamma} + \frac{|d_i(k-1)|^2}{\Lambda}\right]}}$$

for DPD. (28)

IV. CPD Phase Noise Distribution

In Section III, we derived the distribution of the phase difference between the received signal and the reference signal which is the one-symbol delayed version of the received signal perturbed by AWGN plus CCI. On the other hand, the reference signal for CPD is noise free and has an infinite SNIR. This implies that the CPD phase noise distribution can be obtained from the DPD phase noise distribution by letting $\rho(k-1) \to \infty$. It can be shown from (8) that $\rho(k-1) \to \infty$ is equivalent to $\alpha(k-1) \to \infty$. Letting $\alpha(k-1) \to \infty$ in

$$a^2 - b^2 - c^2 = \left(w^2 + 2u\frac{1+l}{\Gamma} + \left(\frac{1+l}{\Gamma}\right)^2\right) \cdot \left[1 - \mathrm{Re}^2\left(\frac{w + \frac{1+l}{\Gamma}(r + j\lambda)\exp -j\Delta\phi_s}{\sqrt{w^2 + 2u\frac{1+l}{\Gamma} + \left(\frac{1+l}{\Gamma}\right)^2}}\exp -j\psi\right)\right]$$

$$\sqrt{a^2 - c^2} \mp b = \sqrt{w^2 + 2u\frac{1+l}{\Gamma} + \left(\frac{1+l}{\Gamma}\right)^2} \cdot \left[1 \pm \mathrm{Re}\left(\frac{w + \frac{1+l}{\Gamma}(r + j\lambda)\exp -j\Delta\phi_s}{\sqrt{w^2 + 2u\frac{1+l}{\Gamma} + \left(\frac{1+l}{\Gamma}\right)^2}}\exp -j\psi\right)\right] \quad (21)$$

$$\overline{F}(\psi|\Delta\phi_s, \boldsymbol{\phi}_i, \Delta T) = \frac{1}{2}\left[-\mathrm{sgn}\,\psi\left(1 - \frac{|\psi|}{\pi}\right) - L\sum_{l=0}^{l-1}\binom{L-1}{l}\frac{(-1)^l}{1+l}\frac{\mathrm{Im}\,(\eta_l \exp -j\psi)}{\sqrt{1 - \mathrm{Re}^2(\eta_l \exp -j\psi)}} \times \frac{2}{\pi}\tan^{-1}\sqrt{\frac{1 + \mathrm{Re}(\eta_l \exp -j\psi)}{1 - \mathrm{Re}(\eta_l \exp -j\psi)}}\right] \quad (25)$$

$$P(\psi|\Delta\phi_s, \boldsymbol{\phi}_i, \Delta T) = \frac{1}{2}\left[1 + \frac{\psi}{\pi} - L\sum_{l=0}^{L-1}\binom{L-1}{l}\frac{(-1)^l}{1+l} \times \left\{\frac{\mathrm{Im}\,(\eta_l \exp -j\psi)}{\sqrt{1 - \mathrm{Re}^2\,(\eta_l \exp -j\psi)}}\frac{2}{\pi}\tan^{-1}\sqrt{\frac{1 + \mathrm{Re}\,(\eta_l \exp -j\psi)}{1 - \mathrm{Re}\,(\eta_l \exp -j\psi)}} + \frac{\mathrm{Im}\,(\eta_l)}{\sqrt{1 - \mathrm{Re}^2\,(\eta_l)}}\frac{2}{\pi}\tan^{-1}\sqrt{\frac{1 - \mathrm{Re}\,(\eta_l)}{1 + \mathrm{Re}\,(\eta_l)}}\right\}\right] \quad (26)$$

(23) and using (9), we obtain

$$\eta_l = \frac{\alpha(k)}{\sqrt{\alpha^2(k) + \dfrac{1+l}{\Gamma}}} = \frac{1}{\sqrt{1 + (1+l)\left[\dfrac{1}{\Gamma} + \dfrac{|d_i(k)|^2}{\Lambda}\right]}} \quad \text{for CPD.} \tag{29}$$

Substitution of (29) into (26) and (27) and recognizing $\mathrm{Im}(\eta_l) = 0$, we obtain the phase noise distribution of coherently detected phase noise θ. It should be pointed out that the CPD phase noise distribution is not affected by the desired signal modulation at all.

V. Discussion

A. Comparison Between DPD and CPD

It is interesting to compare the DPD and CPD phase noise distributions. Substituting (9) into (28) and (29), η_l can be approximated as (30) for large values of Γ and Λ. If $\Lambda \to \infty$, the phase noise is produced due only to AWGN. We call this channel the AWGN-limited channel. In this case, $\eta_l \sim 1 - (1+l)/\Gamma$ for DPD while $1 - (1+l)/(2\Gamma)$ for CPD. Therefore, the distribution for DPD can be approximated as that for CPD with 3-dB reduced SNR. This suggests that the BER performance of DPSK is approximately 3 dB inferior to that of CPSK regardless of the modulation level. On the other hand, if $\Gamma \to \infty$, the phase noise is produced due only to CCI. We call this channel the CCI-limited channel. In this case, η_l is affected by the transmitted CCI symbol sequence through $d_i(k)$ and $d_i(k-1)$, but in different ways for DPD and CPD. So comparison of the phase noise distributions is not simple. Instead, a comparison of the BER performances is presented in Section VI. In the following, the phase noise distributions for three special cases are presented: 1) AWGN-limited channel ($\Lambda \to \infty$), 2) CCI-limited channel ($\Gamma \to \infty$), and 3) unmodulated CCI.

B. Special Cases

1) AWGN-limited channel: η_l becomes

$$\eta_l \to \begin{cases} \dfrac{1}{1 + \dfrac{1+l}{\Gamma}} & \text{for DPD} \\ \dfrac{1}{\sqrt{1 + \dfrac{1+l}{\Gamma}}} & \text{for CPD, as } \Lambda \to \infty. \end{cases} \tag{31}$$

Substituting this into (26), we obtain (32a) and (32b). Pauw and Schilling [8] derived the distributions for DPD and CPD for no diversity case ($L = 1$). We can show that (32a) and (32b) are identical to their results, but our expressions cover the entire range of the phase of interest, i.e., $-\pi \leqq \psi < \pi$.

2) CCI-limited channels:

When $\Gamma \to \infty$, η_l is given by (33), where $\Delta\tilde{\phi}_i = \arg[d_i(k)d_i^*(k-1)]$. Comparison of (31) and (33) shows that for CPD, the faded CCI behaves simply as an AWGN with a power of $I \times |d_i(k)|^2$. In the case of DPD, however, the distribution is influenced further by the modulation phase difference between the desired signal and the CCI. When the CCI is modulated with $\Delta T = 0$ by random sequence of equiprobable M symbols, $\Delta\tilde{\phi}_i$ is equal to $\Delta\phi_i$ and it takes on one of M values from the set $\{2m\pi/M; m = -M/2, \pm(M/2-1), \pm(M/2-2), \cdots, \pm 2, \pm 1, 0\}$. If $\Delta T \neq 0, \Delta\tilde{\phi}_i$ spreads around $\Delta\phi_i$ due to ISI, but it is still symmetrically and continuously distributed with respect to any value from the set $\{2m\pi/M; m = -M/2, \pm(M/2-1), \pm(M/2-2), \cdots \pm 2, \pm 1, 0\}$. Taking account the above statistical property of $\Delta\tilde{\phi}_i$, one can find that the DPD phase noise distribution averaged over CCI modulation does not depend on $\Delta\phi_s$. Therefore, letting $\Delta\phi_s = 0$, the distribution can be computed from (34a) and (34b), which should be averaged over all the possible sequences $\boldsymbol{\phi}_i$ (remember that $d_i(\cdot)$ and $\Delta\tilde{\phi}_i$ can be determined from $\boldsymbol{\phi}_i$). As described above, the distribution for DPD is not affected only by $\Delta\tilde{\phi}_i$ distribution but also by $|d_i(k)|$ and $|d_i(k-1)|$, while that for CPD is affected by $|d_i(k)|$ only. Therefore, the DPD phase noise distribution is more sensitive to timing offset than CPD. Furthermore, it should be pointed out that for both DPD and CPD, the phase noise is symmetrically distributed around its center which is 0 (this

$$P(\psi|\Delta\phi_s, \boldsymbol{\phi}_i, \Delta T) = \frac{1}{2}\left[1 + \frac{\psi}{\pi} - L\sum_{l=0}^{L-1}\binom{L-1}{l}\frac{(-1)^l}{1+l} \times \left\{ \frac{\mathrm{Im}(\eta_l \exp -j\psi)}{\sqrt{1 - \mathrm{Re}^2(\eta_l \exp -j\psi)}}\left(\frac{1}{2} + \frac{1}{\pi}\tan^{-1}\frac{\mathrm{Re}(\eta_l \exp -j\psi)}{\sqrt{1 - \mathrm{Re}^2(\eta_l \exp -j\psi)}}\right) + \frac{\mathrm{Im}(\eta_l)}{\sqrt{1 - \mathrm{Re}^2(\eta_l)}}\left(\frac{1}{2} + \frac{1}{\pi}\tan^{-1}\frac{-\mathrm{Re}(\eta_l)}{\sqrt{1 - \mathrm{Re}^2(\eta_l)}}\right) \right\}\right] \tag{27}$$

$$\eta_l \approx \begin{cases} 1 - \dfrac{1+l}{\Gamma} - \dfrac{1+l}{2\Lambda}[|d_i(k)|^2 + |d_i(k-1)|^2 - 2d_i(k)d_i^*(k-1)\exp -j\Delta\phi_s] & \text{for DPD} \\ 1 - \dfrac{1+l}{2\Gamma} - \dfrac{1+l}{2\Lambda}|d_i(k)|^2 & \text{for CPD} \end{cases} \tag{30}$$

can be easily understood from $P(-\psi) = 1 - P(\psi)$; see (32) and (34)).

3) Unmodulated CCI:

If the CCI is unmodulated ($\Delta\phi_i = 0$), the phase noise distribution can also be expressed as (34), but with $|d_i(k)| = |d_i(k-1)| = 1$ and with $\Delta\tilde{\phi}_i$ replaced by $-\Delta\phi_s$ which takes on one of M values from the set $\{2m\pi/M; m = -M/2, \pm(M/2-1), \pm(M/2-2), \cdots, \pm 2, \pm 1, 0\}$. As a result, when averaged over all transmissions of equiprobable M values of $\Delta\phi_s$, the phase noise distribution becomes identical with that for the modulated CCI case with $\Delta T = 0$.

VI. Error Rate Calculation

First we present BER expressions for 2–16 DPSK/CPSK's using the derived phase noise distribution. When modulation timing offset exists between the desired signal and the CCI, the CCI samples suffer from ISI, which is a function of overall channel filter response. Assuming square root raised cosine filtering, we investigate the impact of modulation timing offset and filter rolloff factor. Finally, we discuss the accuracy of a BER approximation.

A. BER Expression Using Phase Noise Distribution

The BER depends on the rule used to map $\log_2 M$-bit symbol to the carrier phase. The error region of $\Delta\theta$ and θ ranging from $-\pi$ to π is divided into M error regions $\{A_m; m = \pm M/2, \pm(M/2-1), \cdots, \pm 2, \pm 1\}$. We have $A_{m=-M/2} = [-\pi, -(M-1)\pi/M), A_{m=M/2} = [(M-1)\pi/M, \pi)$ and $A_m = [(2m-1)\pi/M, (2m+1)\pi/M)$ for $m \neq \pm M/2$ and 0. The BER can be exactly evaluated from (35), where H_m is the Hamming distance between the incorrect symbol corresponding to the mth error region A_m and the transmitted symbol. $P(\psi)$ is the phase noise distibution given by (26) or (27). It can be seen from Fig. 2 that in the case of $M = 4, H_{m=\pm 2} = 2$ and $H_{m=\pm 1} = 1$ irrespective of the transmitted symbols. For $M = 8$, we can find from Fig. 2 that $H_{m=\pm 4} = H_{m=\pm 2} = 2$ and $H_{m=\pm 1} = 1$, while $H_{m=\pm 3}$ depends on which symbol was transmitted. $H_{m=3} = 1$ and $H_{m=-3} = 3$ for four 3-bit symbols (111), (010), (001), and (100), and $H_{m=3} = 3$ and $H_{m=-3} = 1$ for the other four symbols. Assuming equiporbable transmission of 8 symbols, the averages of $H_{m=3}$ and $H_{m=-3}$ are both equal to 2 bits. In a similar way, we can find the H_m for $M = 16$. Since both $\Delta\theta$ and θ are symmetrically distributed with respect to 0 (see Section V), the BER's for $M = 2$–16 can be exactly evaluated from

$$P_b = \begin{cases} 2P\left(\psi = -\frac{\pi}{2}\right), & M = 2 \\ P\left(\psi = -\frac{\pi}{4}\right) + P\left(\psi = -\frac{3\pi}{4}\right), & M = 4 \\ \frac{2}{3}\left[P\left(\psi = -\frac{\pi}{8}\right) + P\left(\psi = -\frac{3\pi}{8}\right)\right], & M = 8. \\ \frac{1}{4}\begin{bmatrix} 2P\left(\psi = -\frac{\pi}{16}\right) + 2P\left(\psi = -\frac{3\pi}{16}\right) \\ +P\left(\psi = -\frac{9\pi}{16}\right) + P\left(\psi = -\frac{11\pi}{16}\right) \\ -P\left(\psi = -\frac{13\pi}{16}\right) - P\left(\psi = -\frac{15\pi}{16}\right) \end{bmatrix}, & M = 16 \end{cases} \tag{36}$$

$$P(\psi) = \frac{1}{2}\left[1 + \frac{\psi}{\pi} + L\sum_{l=0}^{L-1}\binom{L-1}{l}\frac{(-1)^l}{1+l} \times \frac{\sin\psi}{\sqrt{\left(1+\frac{1+l}{\Gamma}\right)^2 - \cos^2\psi}}\frac{2}{\pi}\tan^{-1}\sqrt{\frac{1+\frac{1+l}{\Gamma}+\cos\psi}{1+\frac{1+l}{\Gamma}-\cos\psi}}\right] \quad \text{for DPD} \tag{32a}$$

$$P(\psi) = \frac{1}{2}\left[1 + \frac{\psi}{\pi} + L\sum_{l=0}^{L-1}\binom{L-1}{l}\frac{(-1)^l}{1+l} \times \frac{\sin\psi}{\sqrt{\frac{1+l}{\Gamma}+\sin^2\psi}}\frac{2}{\pi}\tan^{-1}\frac{\sqrt{1+\frac{1+l}{\Gamma}}+\cos\psi}{\sqrt{\frac{1+l}{\Gamma}+\sin^2\psi}}\right] \quad \text{for CPD.} \tag{32b}$$

$$\eta_l \to \begin{cases} \dfrac{1+\frac{1+l}{\Gamma}|d_i(k)d_i^*(k-1)|\exp -j(\Delta\phi_s - \Delta\tilde{\phi}_i)}{\sqrt{1+\frac{1+l}{\Lambda}|d_i(k)|^2}\sqrt{1+\frac{1+l}{\Lambda}|d_i(k-1)|^2}} & \text{for DPD} \\ \dfrac{1}{\sqrt{1+\frac{1+l}{\Lambda}|d_i(k)|^2}} & \text{for CPD, as } \Gamma \to \infty \end{cases} \tag{33}$$

B. Calculation Procedure

For cellular systems, the CCI comes from spatially separated cochannel cells whose modulation timing may not be synchronized with the desired cell. The modulation timing offset can be assumed uniformly distributed over $[-T/2, T/2)$. When $\Delta T \neq 0$, the sampling timing for the CCI is offset from the ideal timing; hence $d_i(k) \neq \exp j\,\phi_i(k)$ and it contains ISI from several adjacent symbols, see (6). The ISI is given by $\exp[j\,\phi_i(k+m)]\,h(\Delta T - mT), m \neq 0$, and its magnitude with $m > 0 (<0)$ generally becomes larger as ΔT varies from 0 to $0.5T(-0.5T)$ (note that $h(\Delta T - mT) = 0$ if $\Delta T = 0$). The overall filter response $h(t)$ we consider is that of the popular raised cosine filter

$$h(t) = \frac{\sin \pi t/T}{\pi t/T} \frac{\cos \nu \pi t/T}{1 - (2\nu t/T)^2} \tag{37}$$

where ν is the rolloff factor ($0 \leqq \nu \leqq 1$). It is found from (37) that when $\nu = 0.5$ the value of $|h(T/2 - mT)|$ is -4.4 dB, -18.4 dB, and -35.3 dB for $m = 1$, 2, and 3, respectively. From this, the immediately adjacent symbol may be sufficient to consider for BER computation. Here, however, we take into account ISI from two adjacent symbols on each side.

We assume the zeroth symbol $\Delta\phi_s(0)$ is to be detected. As discussed in Section V, the phase noise distribution averaged over all cochannel symbol sequences does not depend on which symbol was transmitted on the desired channel. Without loss of generality, therefore, we can assume $\Delta\phi_s(0) = 0$. The BER calculation is done as follows.

1) Generate the cochannel phase sequence $\boldsymbol{\phi}_i = (\phi_i(-3), \phi_i(-2), \phi_i(-1), \phi_i(0), \phi_i(1), \phi_i(2))$.
2) Compute the values of $d_i(0)$ and $d_i(-1)$ using (6) and (37) for the given ΔT and ν, and substitute them into (28) and (29) to obtain η_l for the given Γ and Λ.
3) Compute the conditional BER using (26) or (27) and (36).
4) Finally, average the conditional BER's over all phase sequences $\boldsymbol{\phi}_i$.

C. Influence of Timing Offset

We consider the CCI-limited channel, i.e., $\Gamma \to \infty$. The calculated BER's of 8DPSK/CPSK in CCI-limited channel with $\Lambda = 20$ dB are plotted as a function of ΔT for various values of ν in Fig. 3. The BER of DPSK is maximized at $\Delta T = 0$ and minimized at $\Delta T = \pm T/2$; when $L = 2$ and $\nu = 1$, for example, one order of magnitude difference is observed. However, for CPSK, the BER's are nearly constant over $\Delta T = -T/2$ to $T/2$ for small values of ν (say,

$$P(\psi|\boldsymbol{\phi}_i, \Delta T) = \frac{1}{2} \cdot \left[1 + \frac{\psi}{\pi} + L \sum_{l=0}^{L-1} \binom{L-1}{l} \frac{(-1)^l}{1+l} \sin\psi \right] \times \left\{ \frac{2}{\pi} \tan^{-1} \frac{\sqrt{\left(1 + \frac{1+l}{\Lambda}|d_i(k)|^2\right)\left(1 + \frac{1+l}{\Lambda}|d_i(k-1)|^2\right) - \left(\cos\psi + \frac{1+l}{\Lambda}|d_i(k)d_i(k-1)|\cos(\psi - \Delta\tilde{\phi}_i)\right)^2}}{\sqrt{\left(1 + \frac{1+l}{\Lambda}|d_i(k)|^2\right)\left(1 + \frac{1+l}{\Lambda}|d_i(k-1)|^2\right) + \cos\psi + \frac{1+l}{\Lambda}|d_i(k)d_i(k-1)|\cos(\psi - \Delta\tilde{\phi}_i)}} \right\} \quad \text{for DPD} \tag{34a}$$

$$P(\psi|\boldsymbol{\phi}_i, \Delta T) = \frac{1}{2} \cdot \left[1 + \frac{\psi}{\pi} + L \sum_{l=0}^{L-1} \binom{L-1}{l} \frac{(-1)^l}{l+1} \frac{\sin\psi}{\sqrt{\frac{1+l}{\Lambda}|d_i(k)|^2 + \sin^2\psi}} \right] \times \frac{2}{\pi} \tan^{-1} \frac{\sqrt{1 + \frac{1+l}{\Lambda}|d_i(k)|^2} + \cos\psi}{\sqrt{\frac{1+l}{\Lambda}|d_i(k)|^2 + \sin^2\psi}} \quad \text{for CPD} \tag{34b}$$

$$P_b = \frac{1}{\log_2 M} \left[\sum_{\substack{m=-(M/2)+1 \\ \neq 0}}^{(M/2)-1} H_m \left[P\left(\psi = (2m+1)\frac{\pi}{M}\right) - P\left(\psi = (2m-1)\frac{\pi}{M}\right) \right] + H_{m=-M/2} P\left(\psi = -(M-1)\frac{\pi}{M}\right) + H_{m=M/2}\left[1 - P\left(\psi = (M-1)\frac{\pi}{M}\right)\right] \right] \tag{35}$$

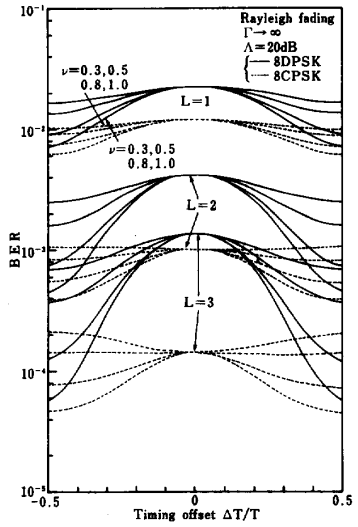

Fig. 3. BER of 8DPSK/CPSK as a function of timing offset ΔT with filter rolloff factor $\nu = 0.3$–1 and number of diversity branches $L = 1$ –3. CCI-limited channel ($\Gamma \rightarrow \infty$).

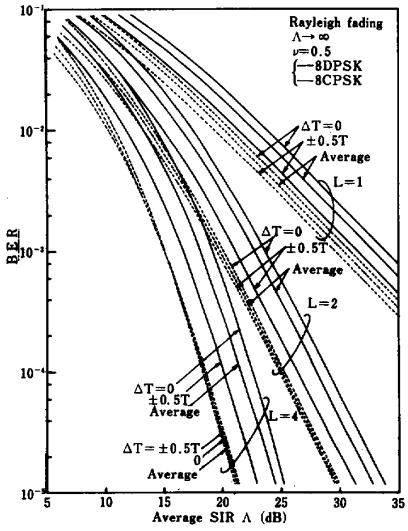

Fig. 4. BER performance of 8DPSK/CPSK as a function of average SIR Λ with timing offset $\Delta T = 0, \pm T/2$ and number of diversity branches $L = 1, 2$, and 4. The BER averaged over uniformly distributed timing offset is also plotted. CCI-limited channel ($\Gamma \rightarrow \infty$).

$\nu = 0.3, -0.5$). Fig. 4 shows the BER performances of 8DPSK/CPSK as a function of average SIR for $\nu = 0.5$. This figure allows us to determine how the required SIR values that achieve BER $= 10^{-3}$ vary according to ΔT. For 8DPSK, by increasing $|\Delta T|$ from zero to $0.5T$, the required SIR reduces by about 2.5 dB when $L = 1$–4. For 8CPSK, however, variations in the required SIR are much smaller. As discussed in Section V-B-2, the BER of DPSK is more sensitive to timing offset than that of CPSK.

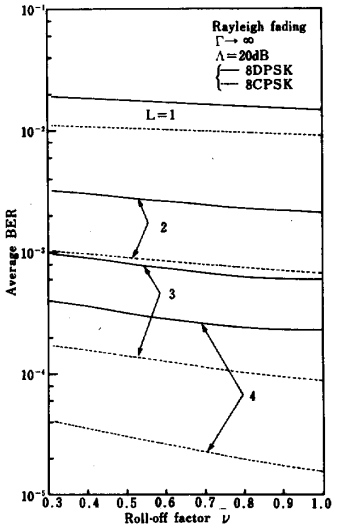

Fig. 5. Average BER of 8DPSK/CPSK as a function of rolloff factor υ with number of diversity branches $L = 1$–4. CCI-limited channel.

For comparison, the results of BER's averaged over uniformly distributed ΔT are also plotted in Fig. 4 (hereafter, we refer to this BER as *average BER). Average BER performance* of 8CPSK is superior by about 2.5–3 dB to that of 8DPSK when $L = 1$–4 (note that in the case of AWGN-limited channel, performance superiority of CPSK is 3 dB for large SNR).

From the discussion in Section V-B-3, the BER performance with $\Delta T = 0$ is the same as that with unmodulated CCI. It can be observed from Fig. 4 that if the CCI is unmodulated, the BER performance of 8DPSK is degraded by about 1 dB compared with the *average BER performance* when $L = 1$–4. For 8CPSK, however, the degradation varies with the number of diversity branches; it is only about 0.6 dB when $L = 1$ and is even smaller when $L = 2$ –4.

D. Influence of Filter Rolloff Factor

The sampled CCI component is given by $d_i(k) = \Sigma_m \exp[j\,\phi_i(k+m)]\,h(\Delta T - mT)$. The contribution from $\phi_i(k)$, i.e., $\exp[j\,\phi_i(k)]\,h(\Delta T)$, is predominant and is less sensitive to the variations in the rolloff factor ν (this can be easily understood by examining (37)); however, the ISI from the other symbols $\phi_i(k+m), m \neq 0$, is sensitive. For larger $\nu, h(t)$ converges to zero more rapidly. Hence, the ISI decreases as ν increases, resulting in BER reductions. To show this, we plot the average BER's of 8DPSK/CPSK in Fig. 5 as a function of ν.

In Fig. 6 the average BER performances of 8–16DPSK's are plotted as a function of the average SIR for various values of ν. It can be seen from Fig. 6(a) that by increasing ν from 0.3 to 1 the BER performance of 8DPSK improves by about 1 dB for $L = 1$–4. This 1-dB performance improvement can also be observed at other modulation levels (see Fig. 6(b)). We also computed the average BER performances of 8–16 CPSK's and observed a similar performance improvement

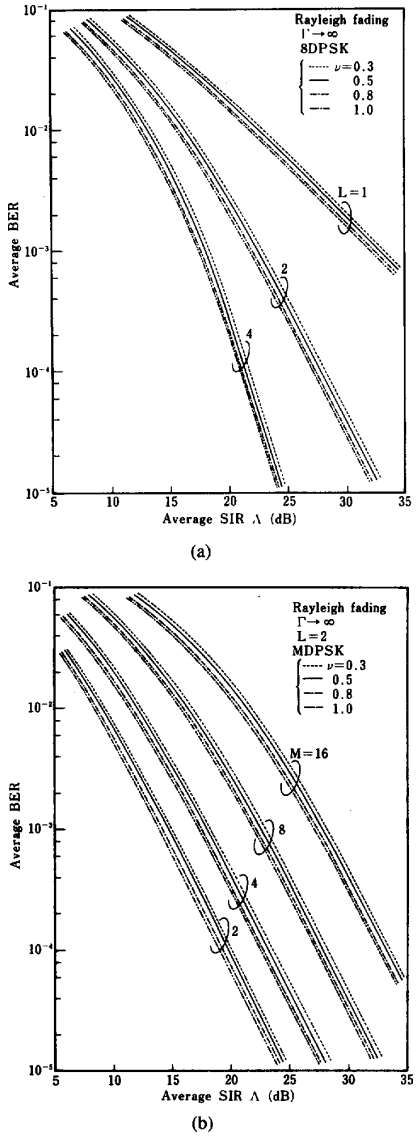

Fig. 6. Average BER performances of 2–16DPSK/CPSK's as a function of average SIR Λ with filter rolloff factor $\nu = 0.3$–1.0. CCI-limited channel ($\Gamma \to \infty$). (a) $M = 8$. $L = 1, 2$, and 4, (b) $M = 2, 4, 8$, and 16. $L = 2$.

achieved by increasing ν (therefore, the computed results are not graphically presented here). However, it should be noted that the BER performance of CPSK is superior to that of DPSK by about 2–3 dB for $M = 2$–16.

Also seen from Fig. 6 is that diversity reception can significantly improve the BER performance due to CCI by using only two antennas ($L = 2$); reduction in the required average SIR at average BER $= 10^{-3}$ is about 10 dB. When L is increased to 4, an additional reduction of 4.5 dB in the required SIR is obtained.

E. BER Performance in the Presence of Both AWGN and CCI

So far, we presented the calculated results in the CCI-limited channel, i.e., errors are caused by CCI only. Here we also consider AWGN. The average BER performances of 2–16 DPSK/CPSK's with $L = 2$ and $\Lambda = 25$ dB are shown in Fig. 7(a) as a function of the average signal energy per bit-to-AWGN power spectrum density ratio $E_b/N_0 (= \mathrm{SNR}/\log_2 M)$. The BER reduces as the average E_b/N_0 increases, but approaches the error floor value due to CCI. In general, the BER performance degrades as the modulation level increases. However, it should be noted that for $E_b/N_0 < 15$ dB (the CCI effect can be neglected), 2 and 4 CPSK have almost identical performance and the 4DPSK performance is only slightly (about 0.5 dB) degraded from 2DPSK. Fig. 7(b) shows the average BER performances of 8DPSK/CPSK for various diversity branch numbers.

F. Approximated BER

It is well known that for high SNR in nonfading environments, the probability of the phase falling in error regions other than the nearest region $A_{m=\pm 1}$ is negligible. With Gray encoding, the nearest error region has a Hamming distance of 1-bit, and therefore,

$$P_b \approx \frac{2}{\log_2 M} P\left(\psi = -\frac{\pi}{M}\right) \tag{38}$$

for the nonfading case. Equation (38) appears as the first term of (36). In Rayleigh fading environments, most errors are produced when the received signal SNR drops near the noise level or CCI level. In this case, the probability of phase noise falling in error regions other than the nearest region may not be negligible. The approximate BER's calculated from (38) are plotted in Fig. 7(b) for 8DPSK/CPSK with $\nu = 0.5$. It can be seen that the approximate BER's are slightly smaller than the exact ones when $L = 1$ (no diversity); the approximation errors at average $E_b/N_0 = \Lambda = 25$ dB are about 11%. Therefore, (38) cannot be used for fading channels. However, it can be seen from Fig. 7(b) that when diversity reception is employed, the approximation errors are negligibly small; 1.9 (2.4)%, 0.26 (0.45)%, and 0.035 (0.077)% when $L = 2$, 3, and 4, respectively, for 8DPSK (8CPSK). This good agreement when diversity reception is employed is attributed to the fact that diversity reception can reduce the variations, due to fading, in the desired signal envelope or power and the statistics of the desired signal approaches the nonfading case.

VII. Conclusion

This paper has analyzed the BER performances of 2–16DPSK/CPSK systems with selection diversity in the presence of AWGN and CCI under very slow Rayleigh fading. The impact of the CCI modulation timing offset and that of the overall channel filter response were investigated. CPSK performance is less sensitive to the modulation timing offset than DPSK. For example, when a rolloff factor of 0.5 is used, the required SIR for 8DPSK at BER $= 10^{-3}$ varies by about 2.5 dB as the timing offset increases zero to $0.5T$ while it is less than 1.5 dB for CPSK. We also found that the BER

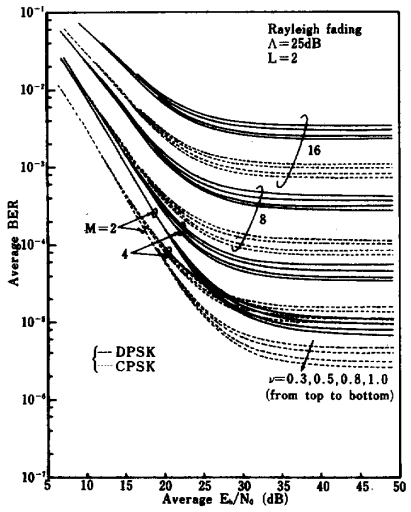

(a)

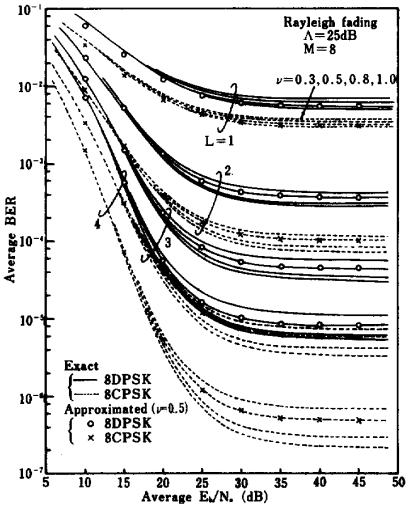

(b)

Fig. 7. Average BER performances of 2–16DPSK/CPSK's as a function of average E_b/N_0 with filter rolloff factor $\nu = 0.3$–1 for average SIR $\Lambda = 25$ dB. (a) $M = 2, 4, 8$ and 16. $L = 2$. (b) $M = 8$. $L = 1$–4.

performance due only to CCI can be improved by about 1 dB by increasing the rolloff factor from 0.3 to 1. The accuracy of the BER approximation was discussed and we found that $2P(\psi = -\pi/M)\log_2 M$ yields accurate BER approximations only when diversity reception is employed. Although our analysis neglected both the effect of fading-induced random phase noise and that of multipath channel delay spread, our results can be useful for the radio link design of digital cellular systems. Extension of our analysis to include the effects of fading-induced random phase noise and delay spread is left for a future study.

Narrowband digital FM is another attractive modulation scheme because of its constant envelope property. For the detection of digital FM signals, either differential phase detection or limiter-discriminator-integrator detection can be used, and therefore the derived phase noise distribution can also be applied to calculate its BER performance.

APPENDIX

For derivation of the phase noise distribution, we use the following two formulas

$$\int_{-(\pi/2)}^{(\pi/2)} \frac{dt}{a + b\cos t + c\sin t} = \frac{4}{\sqrt{a^2 - b^2 - c^2}} \cdot \tan^{-1}\sqrt{\frac{\sqrt{a^2 - c^2} - b}{\sqrt{a^2 - c^2} + b}};\ (a^2 > b^2 + c^2) \tag{A1}$$

$$\frac{1}{2} + \frac{1}{\pi}\tan^{-1}\frac{a}{\sqrt{1 - a^2}} = \frac{2}{\pi}\tan^{-1}\sqrt{\frac{1 + a}{1 - a}}. \tag{A2}$$

The following is the derivation of (A1) and (A2). From [14, eq. (2.559.4)], we obtain

$$\int_{-(\pi/2)}^{(\pi/2)} \frac{dt}{a + b\cos t + c\sin t} = \frac{2}{\sqrt{a^2 - b^2 - c^2}}\left[\tan^{-1}\frac{a - b + c}{\sqrt{a^2 - b^2 - c^2}} + \tan^{-1}\frac{a - b - c}{\sqrt{a^2 - b^2 - c^2}}\right];\ (a^2 > b^2 + c^2). \tag{A3}$$

Applying

$$x + y = 2\tan^{-1}\left(\frac{\sin x + \sin y}{\cos x + \cos y}\right) \tag{A4}$$

to (A3) with

$$x = \tan^{-1}\frac{a - b + c}{\sqrt{a^2 - b^2 - c^2}}, \quad y = \tan^{-1}\frac{a - b - c}{\sqrt{a^2 - b^2 - c^2}} \tag{A5}$$

we obtain (A1). For deriving (A2), we use again (A4). Let $x = \pi/2$ and $y = \tan^{-1} b$. Recognizing $\sin y = b/\sqrt{1 + b^2}$ and $\cos y = 1/\sqrt{1 + b^2}$, we readily obtain

$$\frac{1}{2} + \frac{1}{\pi}\tan^{-1} b = \frac{2}{\pi}\tan^{-1}(b + \sqrt{1 + b^2}). \tag{A6}$$

Finally, letting $b = a/\sqrt{1 - a^2}$, we obtain (A2).

ACKNOWLEDGMENT

The authors wish to thank the anonymous reviewers for their valuable comments and suggestions which helped greatly improve the quality of this paper.

REFERENCES

[1] R. F. Pawula, S. O. Rice, and J. H. Roberts, "Distribution of the phase angle between two vectors perturbed by Gaussian noise," *IEEE Trans. Commun.*, vol. COM-30, pp. 1828–1841, Aug. 1982.

[2] R. F. Pawula, "Asymptotics and error rate bounds for M-ary DPSK, *IEEE Trans. Commun.*, vol. COM-32, pp. 93–94, Jan. 1984.

[3] W. C. Jakes, Jr., *Microwave Mobile Communications*. New York: Wiley, 1974.

[4] M. Hata, K. Kinoshita, and K. Hirade, "Radio link design of cellular land mobile communication systems," *IEEE Trans. Veh. Technol.*, vol. VT-28, pp. 25–31, Feb. 1982.

[5] W. C. Y. Lee, "Spectrum efficiency in cellular," *IEEE Trans. Veh. Technol.*, vol. 38, pp. 69–75, Feb. 1989.

[6] K. Raith and J. Uddenfeldt, "Capacity of digital cellular TDMA systems," *IEEE Trans. Veh. Technol.*, vol. 40, pp. 323–332, May 1991.

[7] Y. Miyagaki, N. Morinaga, and T. Namekawa, "Error probability considerations for M-ary DPSK signal in land mobile radio" (in Japanese), *Trans. IEICE Japan*, vol. J62-B, pp. 581–588, June 1979.

[8] C. K. Pauw and D. L. Schilling, "Probability of error for M-ary PSK and DPSK on a Rayleigh fading channel," *IEEE Trans. Commun.*, vol. 36, pp. 755–756, June 1988.

[9] F. Adachi and M. Sawahashi, "Differential phase noise distribution of Rayleigh faded DPSK signal with selection diversity," *Electron. Lett.*, vol. 28, pp. 898–900, May 1992.

[10] J. G. Proakis, "Probabilities of error for adaptive reception of M-phase signals," *IEEE Trans. Commun. Technol.*, vol. COM-16, pp. 71–81, Feb. 1968.

[11] J. Horikoshi, "Error performance improvement of QDPSK in the presence of cochannel or multipath interference using diversity" (in Japanese), *Trans. IEICE Japan*, vol. J62-B, pp. 24–31, Jan. 1984.

[12] F. Adachi and K. Ohno, "BER performance of QDPSK with postdetection diversity reception in mobile radio channels," *IEEE Trans. Veh. Technol.*, vol. 40, pp. 237–249, Feb. 1991.

[13] C-L. Liu and K. Feher, "Bit error rate performance of $\pi/4$-DQPSK in a frequency-selective fast Rayleigh fading," *IEEE Trans. Veh. Technol.*, vol. 40, pp. 558–568, Aug. 1991.

[14] I. S. Gradshteyn and I. M. Ryzhik, *Table of Integrals, Series, and Products*. Orlando, FL: Academic Press, 1980.

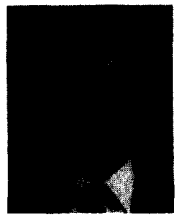

Fumiyuki Adachi (M'79–SM'90) graduated from Tohoku University, Japan, in 1973 and was awarded Dr. Engineering degree from the same university in 1984.

In 1973 he joined the Nippon Telegraph and Telephone Corporation (NTT) Laboratories in Japan, and in 1992 he transferred to NTT Mobile Communications Network, Inc. His major research activities center around mobile communication digital signal processing, including digital modulation/demodulation, diversity reception, channel coding. During the academic year of 1984 to 1985, he was a United Kingdom SERC Visiting Research Fellow at the Department of Electrical Engineering and Electronics of Liverpool University. He is the author of various chapters in three books. He is a corecipient of the 1980 and 1990 IEEE Vehicular Technology Society Paper of the Year Awards.

Dr. Adachi is a member of the Institute of Electronics, Information, and Communication Engineers of Japan.

Mamoru Sawahashi (M'89) was born in Kanagawa, Japan, in 1959. He received the B.S. and M.S. degrees from Tokyo University, Tokyo, Japan.

In 1985 he joined NTT Laboratories, and in 1992 he transferred to NTT Mobile Communication Network, Inc. Since joining NTT, he has been engaged in the research of mobile radio communication systems. He is now a Senior Research Engineer with the Research and Development Department of NTT Mobile Communication Network, Inc.

Mr. Sawahashi is a member of the Institute of Electronics, Information, and Communication Engineers of Japan.